Biosensors and Bioelectronics 25 (2010) 1032–1036

Contents lists available at ScienceDirect

Biosensors and Bioelectronics

journal homepage: www.elsevier.com/locate/bios

Sensing purine nucleoside phosphorylase activity by using silver nanoparticles

Ya Cao[a], Jing Wang[a], Yuanyuan Xu[a], Genxi Li[a,b,*]

[a] Department of Biochemistry and National Key Laboratory of Pharmaceutical Biotechnology, Nanjing University, Nanjing, China
[b] Laboratory of Biosensing Technology, School of Life Science, Shanghai University, 200444 Shanghai, China

ARTICLE INFO

Article history:
Received 11 July 2009
Received in revised form 27 August 2009
Accepted 14 September 2009
Available online 22 September 2009

Keywords:
Purine nucleoside phosphorylase
Silver nanoparticle

ABSTRACT

In this paper, an electrochemical biosensor to assay purine nucleoside phosphorylase (PNP) activity is reported. Due to the facilitation of sliver nanoparticles, which are modified on an electrode surface, to the electron transfer reactivity of guanosine and guanine, the electrochemical response of these species can clearly reveal the activity of the enzyme PNP. This electrochemical biosensor for the assay of PNP activity may have a broad linear range of 4–20 unit/mL with a detection limit of 0.1 unit/mL, which is good enough for clinical applications. Meanwhile, on the basis of the finding that guanosine and guanine can induce silver nanoparticles to different agglomeration degrees, we have also developed a rapid UV–vis spectroscopy assay method for PNP activity. This work may show acceptable reliability and specificity for the assay of PNP activity, and may avoid the utilization of coupled enzymes or radiochemical reagents, which are required to the previous reports.

1. Introduction

Purine nucleoside phosphorylase (PNP, E.C.2.4.2.1) catalyzes the reversible cleavage of the glycosidic bond of natural ribo- and 2′-deoxyribonucleosides, generating the corresponding base and ribose (deoxyribose)-1-phosphate (Bzowska et al., 2000; Montgomery, 1993). Interest in PNP arises from its key role in the purine salvage pathway that enables the cells to utilize purine bases to synthesize purine nucleotides, and from its role in T-cell development (Bzowska et al., 2000; Deng et al., 2006; Montgomery, 1993; Pui and Jeha, 2007; Silva et al., 2007). Human PNP is also a target for T-cell diseases, such as T-cell leukemia and T-cell related autoimmune diseases. Inhibition of PNP may lead to the growth inhibition of activated T-cells, providing a potential therapy for T-cell proliferative disorders.

Up to now, many efforts have been made for the assay of PNP activity (Adam et al., 1998; Kalckar, 1947; Stoeckler and Parks, 1985; Wierzchowski et al., 1996, 2002). The most widely used method proposed by Kalckar is based on the couple of xanthine oxidase, which oxidizes the hypoxanthine released by phosphorolysis of inosine to uric acid. The addition of coupled enzyme is able to significantly improve the sensitivity of the detection approach; however, it may complicate the studies of kinetics and inhibitors of PNP. In recent years, several reports have addressed some new methods to detect PNP activity (Adam et al., 1998; Wierzchowski et al., 1996, 2002). Nevertheless, some of their limitations have restricted their further development in clinical applications, such as low sensitivity and selectivity, or the requirement of radiochemical and fluorescent regents. Hence, simple, sensitive and selective methods are urgently required for the assay of PNP activity.

Nowadays, nanomaterials have been widely employed in biological and biomedical applications (Das et al., 2006; De et al., 2008; Erdem, 2007; Ghadiali and Stevens, 2008; Penn et al., 2003; Polsky et al., 2006; Shen et al., 2008; Wang et al., 2009). Among the nanomaterials, sliver nanoparticles (Ag NPs) exhibit high extinction coefficients and are capable of facilitating electron transfer reactivity of some biological molecules, which will be greatly helpful for their electrochemical applications. Meanwhile, Ag NPs have environment-dependent optical properties, that is, an intense absorption peak at around 390–420 nm arising from surface plasmon resonance, which is sensitive to the surrounding environment (Mulvaney, 1996). Therefore, this nanomaterial is feasible for both electrochemical and optical studies and has received significant research interest (Basu et al., 2008; Braun et al., 2007; Chen et al., 2008; Isse et al., 2006; Lin et al., 2008; Ling et al., 2008, 2009; Liu et al., 2005, 2006; McFarland and Van Duyne, 2003; Ren et al., 2005; Schrand et al., 2008; Thompson et al., 2008; Wei et al., 2008; Xiong et al., 2008; Zhu et al., 2005).

In this work, we have utilized Ag NPs for the development of sensitive and selective sensors to assay PNP activity. An electrochemical biosensor, which is based on the enzymatic reaction concerning the conversion of guanosine to guanine, is firstly proposed with no other enzyme being involved. Meanwhile, we have found that guanine and guanosine can induce Ag NPs into different

* Corresponding author at: Department of Biochemistry and National Key Laboratory of Pharmaceutical Biotechnology, Nanjing University, 22 Hankou Road, 210093 Nanjing, China. Fax: +86 25 83592510.
E-mail address: genxili@nju.edu.cn (G. Li).

0956-5663/$ – see front matter © 2009 Elsevier B.V. All rights reserved.
doi:10.1016/j.bios.2009.09.021

agglomeration degrees, resulting in distinctive absorption spectra changes. On the basis of this finding, a rapid and simple UV–vis spectroscopy assay method for PNP activity has been also proposed in this paper.

2. Materials and methods

2.1. Chemicals and materials

Silver nitrate, trisodium citrate, and sodium borohydride were purchased from Nanjing Chemical Reagent Co., Ltd. (Nanjing, China). Guanosine, human hemoglobin, bovine serum albumin (BSA), and α-thrombin from human plasma were obtained from Sigma–Aldrich. Guanine was from AMRESCO. PNP was purchased from Shanghai Diazyme Co., Ltd. (Shanghai, China). All other reagents were of analytical reagent grade and used as received.

All the buffers were prepared by double-distilled water, which was purified with a Milli-Q purification system (Branstead, USA) to a specific resistance of 18 MΩ cm. The reaction buffer for the enzymatic reaction was 30 mM phosphate buffer solution (PBS), pH 6.5. The termination buffer was 3.5 M $(NH_4)_2SO_4$.

2.2. Apparatus

Electrochemical experiments were carried out on a model 430a Electrochemical Analyzer (CH Instruments, USA) with a conventional three-electrode cell at room temperature. A saturated calomel electrode (SCE) served as the reference electrode, and a platinum wire as the counter electrode. The working electrode was a pyrolytic graphite (PG) electrode. UV absorption spectra were obtained with a UV-2450 UV–vis spectrophotometer (Shimadzu Co., Japan). Transmission electron micrographs were taken using a Jeol JEM-1010 (Jeol Ltd., Tokyo, Japan).

2.3. Preparation and characterization of Ag NPs

Ag NPs were prepared by borohydride reduction of $AgNO_3$ (Doty et al., 2005; Wei et al., 2008). Briefly, 100 mL of the solution containing 0.25 mM $AgNO_3$ and 0.25 mM trisodium citrate was freshly prepared at room temperature. Then an aqueous solution of $NaBH_4$ (6 mL, 5 mM) was added into the above solution under vigorous stirring. After being stirred for 30 min, the prepared Ag NPs were stabilized overnight at room temperature. Transmission electron micrographs and UV–vis spectra were then recorded to characterize the prepared Ag NPs.

2.4. Electrochemical analysis

PG electrode (geometric area: 4.8×10^{-2} cm^2) was prepared as described previously (Zhu et al., 2008). The electrode was firstly polished on rough and fine sand papers and then polished to mirror smoothness with an alumina (particle size of about 0.05 μm)/water slurry on silk. Then the electrode was thoroughly washed by ultrasonicating in both double-distilled water and ethanol for ca. 5 min. After that, 20 μL Ag NPs were spread on the electrode surface, covered with an eppendorf tube overnight at room temperature. Finally, the modified electrode was thoroughly rinsed with double-distilled water and ready for use.

A typical electrochemical analysis was performed in following procedures: 2.5 mL of 2 mM guanosine and 15 μL of sample solution, containing PNP with different concentrations were mixed with 2.5 mL of reaction buffer. The enzymatic reaction was stopped by adding 1 mL termination buffer at a predetermined time (5 min after the addition of the sample solution). Then cyclic voltammetry was immediately carried out in the scan range from 0.2 V to 1.4 V. Differential pulse voltammetry was performed by scanning from 0.2 V to 1.3 V. All the experiments were performed at room temperature. All the potentials reported here were versus SCE.

2.5. UV–vis spectroscopy analysis

The optical detection of PNP was carried out as follows. Firstly, 50 μL of 2 mM guanosine and 1 μL of sample solution which contained PNP with different concentrations were added into 49 μL of the reaction buffer. Then, the mixed reaction solution was incubated at room temperature for 5 min. After that, 100 μL of Ag NPs were mixed with the above solution, and the absorbance was measured from 300 nm to 800 nm.

2.6. Experimental conditions optimization

To obtain the optimal experimental conditions of the enzymatic reaction, several parameters were examined.

2.6.1. Reaction buffer

Phosphate buffer solutions with different ion concentrations were investigated and the pH influence upon the reaction was examined.

2.6.2. Reaction temperature

The effect of reaction temperature on the enzymatic reaction was studied in the range from 4 °C to 60 °C.

2.6.3. Reaction time

To examine the influence of reaction time, enzymatic reactions were lasted for different length of time.

3. Results and discussion

3.1. Characterization of silver nanoparticles

The size distributions of the metal particles synthesized in this work have been analyzed by TEM images, showing that at least 80% of the particles are distributed around 7 nm. The absorption spectrum of the as-prepared Ag NPs displays the characteristic absorbance peak at the wavelength of 393 nm (Fig. S.1 in Supplementary data).

3.2. Electrochemical analysis

Ag NPs are able to facilitate the electron transfer reactivity of guanosine and guanine, which will be greatly helpful for the sensitive assay of PNP activity. To demonstrate the effect of Ag NPs on the electron transfer reactivity of guanosine, bare PG electrode and Ag NPs-modified PG electrode have been separately employed for the electrochemical studies. Fig. 1 shows the cyclic voltammograms of 30 mM PBS (pH 6.5) containing 1 mM guanosine. As is shown in curves a and b, the peak current obtained at the Ag NPs-modified electrode is much higher. In the further control experiment, the cyclic voltammogram of 30 mM PBS (pH 6.5) containing no guanosine which is also obtained at the Ag NPs-modified PG electrode does not show any voltammetric response (Fig. 1c). Therefore, these experimental results confirm that Ag NPs can facilitate the efficiency of the electron transfer between the electro-active molecules and the electrode.

Fig. 2 depicts the differential pulse voltammograms (DPV) observed upon analyzing the activities of different concentrations of PNP. Well-defined DPV peak of the reactant guanosine is observed at around 1.0 V (Fig. 2a) (Goyal et al., 1997). The peak current of guanosine in the presence of PNP (Fig. 2b) is lower than that in the absence of PNP (Fig. 2a) and decreases gradually with

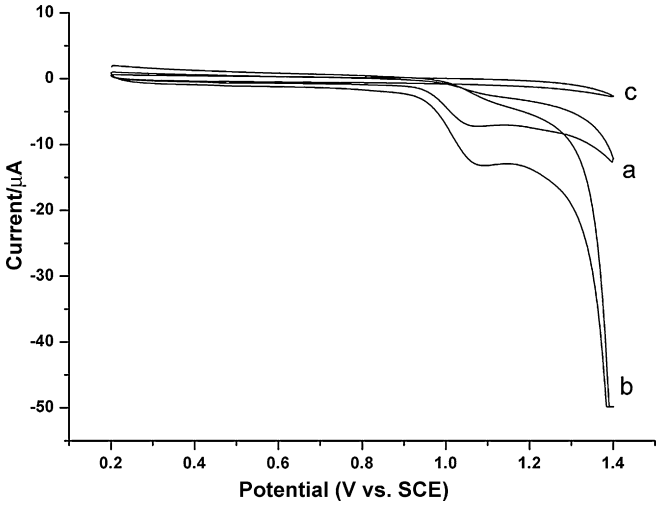

Fig. 1. Cyclic voltammograms obtained at (a) bare PG electrode and (b) Ag NPs-modified PG electrode for 1 mM guanosine. Curve (c) is the case that the test solution contains no guanosine. Scan rate: 0.1 V/s.

the increase of the concentration of PNP (Fig. 2b–i). In the meanwhile, a new peak at around 0.8 V can be observed in the presence of PNP (Fig. 2b–i). According to the literature (Wang et al., 2006), the new peak is contributed to the guanine that is converted from guanosine by PNP. As the concentration of PNP becomes higher, the peak current of the product guanine increases (Fig. 2b–i), consistent with the conversion of elevated amounts of guanosine to guanine. On the other hand, the kinetics of the enzymatic reaction with 10 unit/mL PNP has been monitored by stopping the reaction at different time intervals and measuring the differential pulse voltammograms immediately. As the reaction time is prolonged, more guanosine is converted to guanine, so the corresponding peak currents are changed (Fig. S.2 in Supplementary data). Experimental results reveal that the two peaks keep nearly unchanged after about 10 min. But, due to the reasons that a short-time analysis is highly desired and 5 min is enough for the sensitive detection, we have then chosen 5 min as the optimal reaction time for the electrochemical biosensor.

The calibration curves for the electrochemical biosensor have been shown in Fig. 3. The peak current of the reactant guanosine decreases with the PNP concentration over the range of

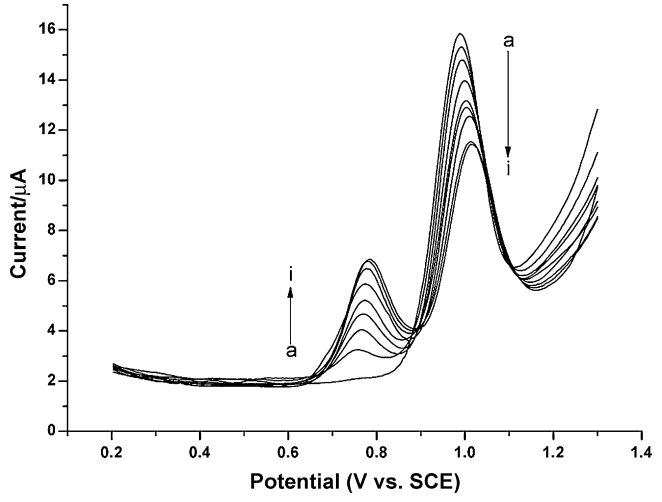

Fig. 2. Differential pulse voltammograms obtained at Ag NPs-modified PG electrode for the electrochemical detection of PNP activity with increasing concentration of the enzyme at (a) 0, (b) 2, (c) 5, (d) 10, (e) 15, (f) 20, (g) 30, (h) 50, (i) 80 unit/mL.

Table 1
Assay results of serum samples by using the proposed electrochemical biosensor and the comparison with the given PNP concentrations in serum samples.

Samples	PNP concentration detected by proposed method (unit/mL)	Standard PNP concentration (unit/mL)	Relative error (%)
1	5.29	5.00	5.8
2	9.86	10.00	1.4
3	20.86	20.00	4.3

0–50 unit/mL, with a linear range of 2–20 unit/mL (Fig. 3A). The linear regression equation is $I = 0.1244$ [PNP] (unit/mL) + 10.7052 ($R^2 = 0.9993$). In the other case, when the peak current of the product guanine is used as the analytical signal, linear dependence can be obtained over the concentration range from 5 unit/mL to 20 unit/mL (Fig. 3B). The linear regression equation is $I = 0.1009$ [PNP] (unit/mL) + 0.8745 ($R^2 = 0.9934$). Furthermore, the detection limit has been also obtained based on the evaluation of the average response of the blank plus three times the standard deviation (Centi et al., 2007). If the peak current of guanosine is used as the analytical signal, the blank signal is 10.75 ± 0.02 μA, leading to a detection limit of 0.1 unit/mL, which is the lowest compared with the previous reports (Adam et al., 1998; Kalckar, 1947; Wierzchowski et al., 1996, 2002). Since the normal level of PNP in human is about 14 unit/mL (erythrocytes) or 6 unit/mL (bloods) (Wierzchowski et al., 2002), the linear range and detection limit of the electrochemical sensor are good enough for clinical applications.

The reliability of the electrochemical biosensor has been estimated with intra- and inter-assay coefficients of variation (CV). The intra-assay CV is evaluated by assaying one PNP level for three replicate measurements. The inter-assay CV is evaluated by determining one PNP level with three replicate samples using the same electrode. Samples containing 10 unit/mL PNP have been used in the reliability evaluation. The intra- and inter-assay CVs are 4.57% and 8.9% for the peak of guanosine, 2.46% and 4.94% for the peak of guanine. So the precision and reliability of the electrochemical biosensor proposed in this work are acceptable.

Moreover, the specificity of the electrochemical biosensor has been also evaluated. We have mixed 10 unit/mL PNP and some other nonspecific proteins, such as 1 mg/mL BSA, 10 μM α-thrombin, and 1 mg/mL human hemoglobin, and have then detected the DPV waves. In comparison with the DPV response obtained from the pure PNP, nearly no significant difference can be observed (Fig. S.3 in Supplementary data). To further demonstrate the applicability of this developed electrochemical biosensor in clinical applications, serum samples have been also employed. Different amounts of PNP were dissolved into human serum, which contained many kinds of nonspecific proteins, to prepare serum sample solutions. The results, which are obtained by using the peak current of guanine as the analytical signal, have been shown in Table 1. The relative errors are less than 6%, so this electrochemical biosensor may provide a useful tool for the detection of PNP in clinical laboratory.

3.3. UV–vis spectroscopy analysis

Ag NPs show an intense absorption peak at around 390–420 nm, arising from surface plasmon resonance. The exact plasmon resonance band is dependent on the size, surrounding environment, and distance of the particles. Upon aggregation of Ag NPs, a significant red shift in absorbance can be observed. Both guanosine and guanine have exocyclic amine groups and are capable of interacting with Ag NPs (Nath et al., 2006). The interaction between Ag NPs and guanosine or guanine leads to the decrease of the interparticle spacing between the nanoparticles. However, the guanosine has an extra ribose group, baffling the decrease of the interparticle

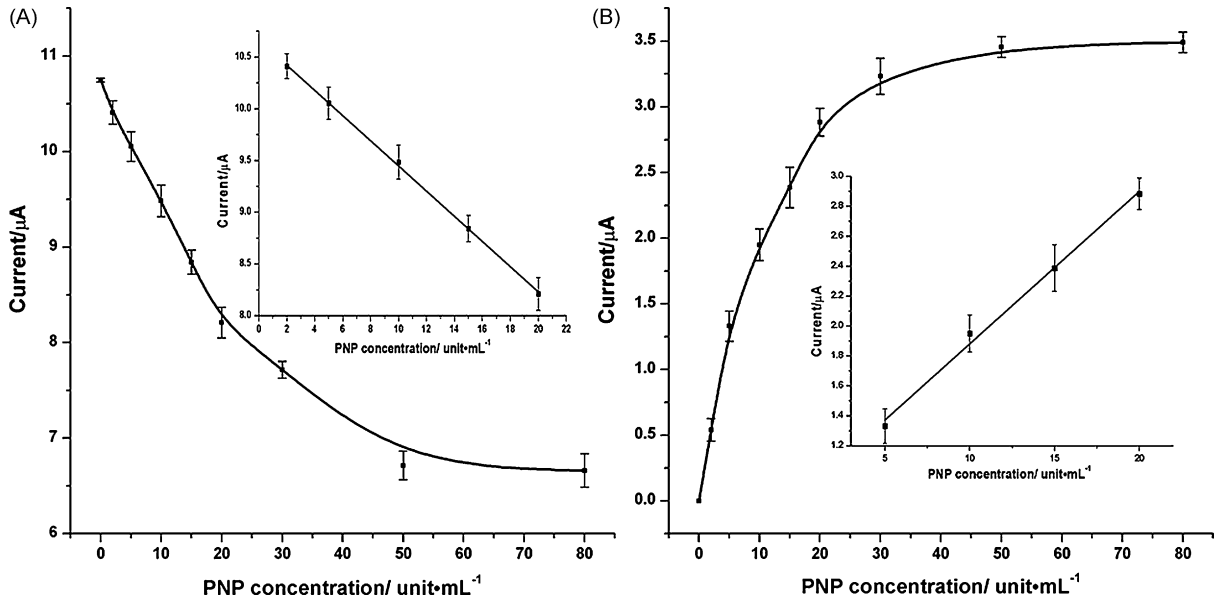

Fig. 3. Dependence of the peak currents of (A) guanosine and (B) guanine on the concentration of PNP. Inset: the linear relationships between the peak currents and the PNP concentration. Error bars represent standard deviations of measurements ($n = 3$).

spacing. Therefore, guanosine and guanine induce Ag NPs to different agglomeration states, resulting in distinctive absorption spectra changes (Fig. 4, curves b and c). On the basis of this, we have also used Ag NPs as optical probes and developed a rapid and simple UV–vis spectroscopy assay method for PNP activity.

Typical UV–vis spectra of test solutions that contain 1 mM guanosine in the presence and absence of PNP have been shown in Fig. 4 (curves b, d and e). As shown in Fig. 4 (curve b), the absorption spectrum of the test solution in the absence of PNP displays a main absorbance peak at the wavelength of 402 nm. Following the addition of PNP, the intensity of the 402-nm peak decreases and shifts to longer wavelength, while the intensity of the spectrum at 800 nm increases (Fig. 4, curves d and e). In the further control experiment, the absorption spectrum of Ag NPs with PNP displays an absorbance peak at the wavelength of 394 nm (Fig. 4, curve a), nearly unchanged compared with that of Ag NPs alone. Obviously, the spectrum change is attributed to the conversion of guanosine to guanine catalyzed by PNP. In further study, the radio of the absorbance at 800 nm to the absorbance at 402 nm (A_{800}/A_{402}) has been chosen to determine the activity of PNP (Li and Rothberg, 2004; Liu and Lu, 2003).

Several important aspects involved in the enzymatic reactions have been examined and optimized (Fig. S.4 in Supplementary data). With the increase of the ion concentration, the A_{800}/A_{402} value increases, and keeps nearly unchanged when the ion concentration is higher than 30 mM. Meanwhile, the highest response can be obtained at pH 6.5. Thus, 30 mM PBS, pH 6.5 is chosen as the reaction buffer, in which PNP possesses the highest catalytic activity. On the other hand, it can be known that the maximum A_{800}/A_{402} value is observed at 25 °C. Furthermore, time courses of the reaction have been performed with several different PNP concentrations. Considering that excessive length of the reaction time may influence the efficiency of a rapid assay and the sensitivity at 5 min is enough, we choose 5 min as the optimal reaction time.

The calibration curve for the UV–vis spectroscopy assay method has been shown in Fig. 5. The A_{800}/A_{402} value increases with the PNP

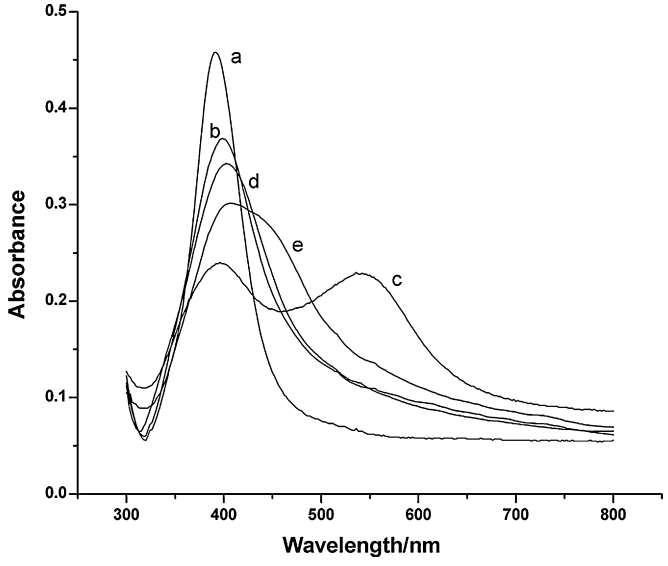

Fig. 4. UV–vis spectra of the mixture of silver nanoparticles and (a) 10 unit/mL PNP, (b) 1 mM guanosine, (c) 1 mM guanine. Curves d and e are the UV–vis spectra observed upon analyzing the activities of 4 unit/mL and 10 unit/mL PNP.

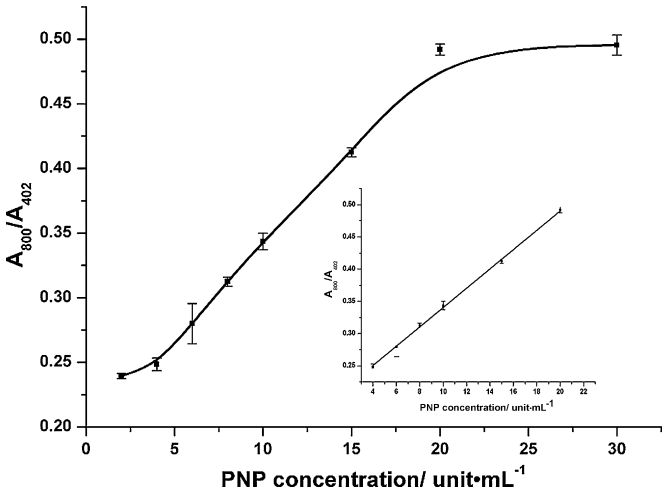

Fig. 5. Calibration curve for the spectrophotometric detection of PNP. Error bars represent standard deviations of measurements ($n = 3$). Inset: The A_{800}/A_{402} value versus the PNP concentration is linear over the range of 4–20 unit/mL.

concentration over the range of 2–30 unit/mL. The inset of Fig. 5 indicates that the A_{800}/A_{402} value versus the PNP concentration is linear over the range of 4–20 unit/mL. Furthermore, the reliability of the UV–vis spectroscopy assay method has been also evaluated by intra- and inter-assay CVs, which are obtained by examining the sample solutions containing 10 unit/mL PNP. The intra- and inter-assay CVs of the UV–vis spectroscopy assay method are separately 0.9% and 2.4%, also showing acceptable reliability.

4. Conclusions

In summary, we have employed Ag NPs to assay PNP activity. And we have proposed both an electrochemical biosensor and an UV–vis spectroscopy assay method for the assay of PNP activity. The UV–vis spectroscopy assay method is less sensitive, yet can be completed in 10 min, revealing simpler configuration. The electrochemical biosensor reveals higher sensitivity compared with the UV–vis spectroscopy assay method and other techniques in the previously published literatures, and has shown successful determination of PNP in serum samples, possessing a promising practicality in clinical diagnosis. Furthermore, both of the electrochemical biosensor and the UV–vis spectroscopy assay method may have broad linear ranges and acceptable reliability, and may avoid the use of either coupled enzymes or radiochemical reagents, which may be of value for investigating the kinetics of PNP and developing novel PNP inhibitors in the future.

Acknowledgements

This work was supported by the National Natural Science Foundation of China (Grant Nos. 90406005, 20575028) and the Program for New Century Excellent Talents in University, the Chinese Ministry of Education (NCET-04-0452).

Appendix A. Supplementary data

Supplementary data associated with this article can be found, in the online version, at doi:10.1016/j.bios.2009.09.021.

References

Adam, T., Sevcik, J., Fairbanks, L.D., Bartak, P., 1998. Adv. Exp. Med. Biol. 431, 759–763.
Basu, S., Jana, S., Pande, S., Pal, T., 2008. J. Colloid Interface Sci. 321, 288–293.
Braun, G., Lee, S.J., Dante, M., Nguyen, T.Q., Moskovits, M., Reich, N., 2007. J. Am. Chem. Soc. 129, 6378–6379.
Bzowska, A., Kulikowska, E., Shugar, D., 2000. Pharmacol. Ther. 88, 349–425.
Centi, S., Tombelli, S., Minunni, M., Mascini, M., 2007. Anal. Chem. 79, 1466–1473.
Chen, Z., Xie, S.B., Shen, L., Du, Y., He, S.L., Li, Q., Liang, Z.W., Meng, X., Li, B., Xu, X.D., Ma, H.W., Huang, Y.Y., Shao, Y.H., 2008. Analyst 133, 1221–1228.
Das, J., Aziz, M.A., Yang, H., 2006. J. Am. Chem. Soc. 128, 16022–16023.
De, M., Ghosh, P.S., Rotello, V.M., 2008. Adv. Mater. 20, 4225–4241.
Deng, H., Murkin, A.S., Schramm, V.L., 2006. J. Am. Chem. Soc. 128, 7765–7771.
Doty, R.C., Tshikhudo, T.R., Brust, M., Fernig, D.G., 2005. Chem. Mater. 17, 4630–4635.
Erdem, A., 2007. Talanta 74, 318–325.
Ghadiali, J.E., Stevens, M.M., 2008. Adv. Mater. 20, 4359–4363.
Goyal, R.N., Jain, N., Garg, D.K., 1997. Bioelectrochem. Bioenerg. 43, 105–114.
Isse, A.A., Gottardello, S., Maccato, C., Gennaro, A., 2006. Electrochem. Commun. 8, 1707–1712.
Kalckar, H.M., 1947. J. Biol. Chem. 167, 429–433.
Li, H.X., Rothberg, L., 2004. Proc. Natl. Acad. Sci. U.S.A. 101, 14036–14039.
Lin, L., Qiu, P.H., Cao, X.N., Jin, L.T., 2008. Electrochim. Acta 53, 5368–5372.
Ling, J., Sang, Y., Huang, C.Z., 2008. J. Pharm. Biomed. Anal. 47, 860–864.
Ling, J., Li, Y.F., Huang, C.Z., 2009. Anal. Chem. 81, 1707–1714.
Liu, C.H., Li, Z.P., Du, B.A., Duan, X.R., Wang, Y.C., 2006. Anal. Chem. 78, 3738–3744.
Liu, J.W., Lu, Y., 2003. J. Am. Chem. Soc. 125, 6642–6643.
Liu, S.H., Zhang, Z.H., Han, M.Y., 2005. Anal. Chem. 77, 2595–2600.
McFarland, A.D., Van Duyne, R.P., 2003. Nano Lett. 3, 1057–1062.
Montgomery, J.A., 1993. Med. Res. Rev. 13, 209–228.
Mulvaney, P., 1996. Langmuir 12, 788–800.
Nath, S., Ghosh, S.K., Kundu, S., Praharaj, S., Panigrahi, S., Pal, T., 2006. J. Nanopart. Res. 8, 111–116.
Penn, S.G., He, L., Natan, M.J., 2003. Curr. Opin. Chem. Biol. 7, 609–615.
Polsky, R., Gill, R., Kaganovsky, L., Willner, I., 2006. Anal. Chem. 78, 2268–2271.
Pui, C.H., Jeha, S., 2007. Nat. Rev. Drug Discov. 6, 149–165.
Ren, X.L., Meng, X.W., Chen, D., Tang, F.Q., Jiao, J., 2005. Biosens. Bioelectron. 21, 433–437.
Schrand, A.M., Braydich-Stolle, L.K., Schlager, J.J., Dai, L.M., Hussain, S.M., 2008. Nanotechnology 19, 235104.
Shen, L., Chen, Z., Li, Y.H., He, S.L., Xie, S.B., Xu, X.D., Liang, Z.W., Meng, X., Li, Q., Zhu, Z.W., Li, M.X., Le, X.C., Shao, Y.H., 2008. Anal. Chem. 80, 6323–6328.
Silva, R.G., Nunes, J.E.S., Canduri, F., Borges, J.C., Gava, L.M., Moreno, F.B., Basso, L.A., Santos, D.S., 2007. Curr. Drug Targets 8, 413–422.
Stoeckler, J.D., Parks Jr., R.E., 1985. Methods Pharmacol. 6, 147–162.
Thompson, D.G., Enright, A., Faulds, K., Smith, W.E., Graham, D., 2008. Anal. Chem. 80, 2805–2810.
Wang, J., Meng, W.Y., Zheng, X.F., Huang, J.Y., Li, G.X., 2009. Biosens. Bioelectron. 24, 1598–1602.
Wang, Z.H., Xiao, S.F., Chen, Y., 2006. J. Electroanal. Chem. 589, 237–242.
Wei, H., Chen, C.G., Han, B.Y., Wang, E.K., 2008. Anal. Chem. 80, 7051–7055.
Wierzchowski, J., Wielgus-Kutrowska, B., Shugar, D., 1996. Biochim. Biophys. Acta 1290, 9–17.
Wierzchowski, J., Ogiela, M., Iwanska, B., Shugar, D., 2002. Anal. Chim. Acta 472, 63–74.
Xiong, D.J., Chen, M.L., Li, H.B., 2008. Chem. Commun., 880–882.
Zhu, X.L., Gan, X., Wang, J., Chen, T., Li, G.X., 2005. J. Mol. Catal. A: Chem. 239, 201–204.
Zhu, X.L., Zhang, W.J., Xiao, H., Huang, J.Y., Li, G.X., 2008. Electrochim. Acta 53, 4407–4413.